WILEY | Hindawi

Research Article

Polylactic Acid-Based Film Modified with Nano-Ag-Graphene-TiO₂: New Film versus Recycled Film

Anca Peter [ID],[1] **Camelia Nicula** [ID],[2] **Anca Mihaly Cozmuta** [ID],[1] **Goran Drazic** [ID],[2] **Antonio Peñas** [ID],[3] **Stefania Silvi** [ID],[4] and **Leonard Mihaly Cozmuta** [ID][1]

[1]*Technical University of Cluj Napoca, Faculty of Sciences, Victoriei 76, 430072, Baia Mare, Romania*
[2]*National Institute of Chemistry, Hajdrihova 19 P.O. Box 660 SI-1001, Ljubljana, Slovenia*
[3]*Andaltec, Pol. Ind. Cañada de la Fuente Vílches s/n, 23600, Martos-Jaén, Spain*
[4]*University of Camerino, School of Bioscience and Veterinary Medicine, Gentile III da Varano, MC 62032, Camerino, Italy*

Correspondence should be addressed to Anca Peter; peterancaluca@yahoo.com

The increase in the polymer-based materials needs has induced along the waste accumulation, thus argued higher interest in recycling. The study aims to assess the structural, morphological, mechanical resistance, physical–chemical and biochemical characteristics, as well as the preservative role during the curd cheese storage of a recycled polylactic acid (PLA)-based film modified with Ag-graphene-TiO₂ nanostructured composite, obtained by recovering the composite from the used film, followed by its incorporation in new PLA. The breaking load of the recycled film was 24% lower than that of the new film and 10% higher than of the neat PLA. Differential scanning calorimetry (DSC) showed changes of the recycled PLA's surface tension and crystallization degree in a greater extent than in the newly prepared film, revealing better incorporation of the recovered composite into the PLA matrix. Fourier transformed infrared spectroscopy showed the formation of C–O–Ti bridges between composite and PLA both in new and recycled film. Oxygen transmission rate (OTR) of the new and recycled film decreased by 33% and 45%, respectively, in comparison with reference PLA. The curd cheese was successfully stored in the recycled packaging; the organoleptic characteristics of cheese wrapped in recycled film were superior in comparison with the new film. The variation of fat and protein contents and mass loss was the lowest when the recycled film was used as packaging material. The study successfully showed the possibility to recover and recycle the used PLA-based films modified with inorganic nanocomposites.

1. Introduction

The sharp and constant increase of waste from nondegradable plastics is a cruel reality, with negative effect over the environmental components. Almost 448 million tons of nondegradable plastics are discarded annually [1], which has prompted the need to find new, efficient, and fast solutions to reduce the plastic environmental impact. Thus, different approaches are under study at lab, pilot, and industrial scale, which are mainly focused on two strategies: (1) using biodegradable materials and (2) recycling.

Concerning biodegradable materials, their main advantage is the short degradability period (a few months), which reduces its persistence in the environment and, consequently, its impact. However, their effectiveness, as food packaging materials, whether are not modified with active compounds, is limited. For example, Ramos et al. [2] showed that the presence of thymol and nano-Ag modifies the thermal, optical, and barrier properties of polylactic acid (PLA) and enhances its disintegration rate, in a higher extend, than in the case of pristine PLA. Zabidi et al. [3] have obtained PLA modified with cellulose and thymol/curry essential oil and they have demonstrated the antimicrobial and preservative activity of the active films during the tomato storage in comparison with the nonmodified PLA. Peter et al. [4] showed that the best preservative role of PLA during the curd storage

was achieved when activating with a content of the active (Ag-graphene-TiO$_2$) composite (in the range of 0.5–3 wt%). Moreover, the study reveals that the mechanical resistance was enhanced by 30% by composite addition. Chi et al. [5] have demonstrated the preservative activity of PLA modified with essential oil, nano-Ag, and nano-TiO$_2$ during the mango storage in comparison with that of neat PLA by delaying the firmness loss, the color, total acidity, and vitamin C depreciation.

The recycled materials are generating lower carbon footprint than the pristine material and are providing unique opportunity to obtain materials with high added value from traditionally materials considered wastes, such as used food packaging. Peter et al. [4] showed that the preservative role of the PLA-based film for curd packaging, after the second use, remained unchanged when the content of the active composite into the PLA was 0.5 wt%. However, whether the percent of the active agent increased to 3 wt%, the active role of the reused film decreased to 85% from the maximum capacity of the new film. Geetha et al. [6] showed that TiO$_2$–SO$_4$ catalysts can be successfully used to piperidine synthesis even five times, the process yield decreasing only by 2%. Menon et al. [7] showed that the photocatalytic removal of estrogenic compounds over the TiO$_2$–ZnO nanocomposite is efficient even after three cycles under visible irradiation without loss in activity.

Plavec et al. [1] showed that PLA-PHB blend can be successfully recycled and the mechanical and thermal properties were not negatively affected. Yan et al. [8] have demonstrated that CeO$_2$–TiO$_2$ nanoarrays could be successfully three times reused and also recycled in the water sterilization process by keeping the same efficacy. Liu et al. [9] reported the recycling capacity of TiO$_2$-based flocs modified with Al and carbonate ions, having petal-like mesoporous structures and relatively high surface area and photoactivity.

Khodanazary and Mohammadzadeh [10] and Izadi et al. [11] obtained active packaging based on PLA modified with whey protein and ZnO nanoparticles [10] and with *Thymus daenensis Celak*, essential oil, beta-cyclodextrin, and nano-Ag, respectively [11], that have been used successfully for fish and beef meat storage. The modified PLA demonstrated a synergistic effect in retarding the microbial growth and is preserving the organoleptical characteristics of the fish meat. Moreover, the efficient entrapment of the essential oil in beta-cyclodextrin extended the shelf life of beef meat.

The novelty of this study lies in the fact that, at present, in the specialized literature, the information about the recyclability of materials based on PLA is extremely low. The importance of the inorganic composite recycling consists of the fact that the precursors used for the Ag-graphene-TiO$_2$ composite's preparation, namely titanium tetraisopropoxide (TEOS), silver nitrate (AgNO$_3$), anhydrous ethanol, and nitric acid (HNO$_3$), are very toxic. In this regard, the possibility of the inorganic composite's recycling will reduce the harmful effect of these substances both over the researcher/worker that is preparing the composite and personal from the company that supplies these reagents. The recycling procedure was applied due to the fact that it is known that by heat treatment at 500°C, the organic matter is charred

and eliminated in the form of CO$_2$ and the composite materials based on TiO$_2$ suffer reduced structural changes. Herein, we report a study aimed to recycle a modified PLA film with Ag, graphene, and TiO$_2$ composite and to establish the variations in structure, morphology, mechanical properties, and preservative activity during the curd cheese storage for a newly prepared and recycled film.

2. Materials and Methods

2.1. Materials. TEOS, HNO$_3$, phenolphthalein, anhydrous potassium sulfate (K$_2$SO$_4$), selenium (Se), hydrochloric acid (HCl), and potassium bromide (KBr) were acquisitioned from Merck (Germany). Ninety-eight percent sulfuric acid (H$_2$SO$_4$) solution was purchased from Lach-Ner, Czech Republic. Anhydrous ethanol (C$_2$H$_5$OH), AgNO$_3$, sodium hydroxide (NaOH), 35% hydrogen peroxide (H$_2$O$_2$), boric acid (H$_3$BO$_3$), and salicylic acid (C$_7$H$_6$O$_3$) were purchased from Chemical Company (Romania). Ultrapure water was used for the gels preparation and was prepared by using an equipment for ultrapure water Thermo Fisher Scientific (USA) device. Graphene powder was GP500 Graphene Nanoplatelets from GrapheneTech (Spain). PLA NatureWorks 4043D (USA) has been used. The molecular weight of PLA 4043D from GPC is 154.378 g/mol [12].

2.2. Preparation of the Nano-Ag-Graphene-TiO$_2$ Composite. The preparation procedure is described in our previous study [4]. The titanium dioxide sol was prepared by the sol–gel method in acidic catalysis by TEOS, ultrapure water, anhydrous ethanol, and 63 wt% HNO$_3$. The molar ratio of the reactants was TEOS:water:ethanol:HNO$_3$ = 1 : 3 : 20 : 0.08. An amount of 0.1 wt% graphene powder was, subsequently, added under continuously magnetic stirring. The obtained black gels were immersed in 0.015 M AgNO$_3$ solution for 24 hr and were dried at 60°C and heat treated at 500°C for 2 hr. A black powder was obtained.

2.3. Preparation of the New Nano-Ag-Graphene-TiO$_2$-PLA Film. The nano-Ag-TiO$_2$-graphene composite was used to develop the Ag-graphene-TiO$_2$-PLA film. A mixture of composite 0.5 wt% and PLA grains was prepared by using the internal mixer equipment at 170°C. The homogenate was, subsequently, cooled down at room temperature. Then, the mixture was extruded with a single screw extruder and the obtained filament was chopped with a pelletizer in order to obtain composite-PLA grains (~2-mm diameter). Subsequently, the composite-PLA film was prepared by blow extrusion at 180°C.

2.4. Storage of the Curd Wrapped in the Nano-Ag-Graphene-TiO$_2$-PLA Film. The nano-Ag-graphene-TiO$_2$-PLA film was used for the curd storage according to the experimental conditions described in our previous studies [4, 13]. The curd cheese was homemade prepared according to the traditional recipe used in the rural households from Northwestern Romania. An amount of 100 g curd cheese was wrapped in a 40 cm/40 cm sheet of nano-Ag-graphene-TiO$_2$-PLA film and the obtained packages were stored under UV-illuminated refrigerator at 4°C. Samples were periodically analyzed in terms of organoleptic and physical–chemical changes (mass loss, titratable acidity, dry mass, fat and protein contents).

The organoleptic changes were monitored according to the Romanian Quality Standard for fresh cheese SR3664:2008. Appearance, consistency, color, flavor, and taste were evaluated and compared with the accepted characteristics.

Mass loss was determined by monitoring the difference of the package mass between day 0 (beginning) and 21 (ending) of the storage experiment.

Titratable acidity was determined by cheese titration with solution 0.1 N NaOH, in the presence of phenol-phthalein 1%, until the pink color persisted at least 30 s.

The fat content was determined by using the solvent extractor VELP Scientifica and anhydrous ethanol was used as solvent. The working temperature was 210°C. The ethanolic solution obtained after extraction was dried in a desiccator until reaching the constant mass.

The protein content was determined by Kjeldahl method by using the VELP Scientifica system. A mixture of 2 g cheese, 7 g anhydrous potassium sulfate, 5 mg selenium, 7 mL 98% H_2SO_4 solution, and 5 mL 35% H_2O_2 was prepared for digestion, which took place at 420°C for 30 min. The distillation was performed in the presence of 35% NaOH. The distillate was combined with 25 mL 4% H_3BO_3. The final titration was performed with 0.2 N HCl in the presence of Tashiro indicator when a color change from green into purple occurred. The protein content was calculated in mg of nitrogen in 1 g of cheese.

2.5. Recycling of the Nano-Ag-Graphene-TiO₂-PLA Film.

The used nano-Ag-graphene-TiO_2-PLA packaging film was cleaned from the curd waste, washed three times with ultrapure water, rinsed for 1 min in anhydrous ethanol, and dried in air for 24 hr. The cleaned film was calcined in Carbolite furnance at 500°C for 4 hr, the temperature increasing rate being 2°C/min. The removal of organic matter occurred during calcination and, finally, the inorganic composite (black powder) was obtained.

Then, the recovered composite was included in new PLA film, according to the procedure presented in section "Preparation of the new nano-Ag-graphene-TiO_2-PLA film."

2.6. Storage of Curd Wrapped in the Recycled Nano-Ag-Graphene-TiO₂-PLA Film.

The recycled nano-Ag-graphene-TiO_2-PLA film was used for the curd storage in identical conditions with those presented in the section "Storage of the curd wrapped in the nano-Ag-graphene-TiO_2-PLA film."

2.7. Characterization of the Nano-Ag-Graphene-TiO₂ Composite.

The nano-Ag-graphene-TiO_2 composite was characterized as follows. Morphology was established by optical and electronic microscopy (scanning transmission electron microscopy (STEM)-high-angle annular dark field (HAADF)). Structure was determined by performing Fourier transformed infrared spectroscopy (FTIR) and X-ray diffraction (XRD) and by determining elemental composition by energy-dispersive X-ray spectroscopy (EDXS). The optical analysis was evaluated by performing UV–vis spectroscopy, and the gap energy was calculated by using the Kubelka–Munk equation. The thermal stability of the composite was determined by thermogravimetric analysis (TGA)/differential scanning calorimetry (DSC). The photoactivity of the composite was carried out during the photodegradation of salicylic acid under UV light illumination. The specification of the abovementioned procedures is described in detail in our previous study [4].

2.8. Characterization of New and Recycled Nano-Ag-Graphene-TiO₂-PLA Film.

The scanning electron microscopy (SEM) was performed according to the method described in our previous study [4]. The STEM measurements were performed using a JEOL ARM 200CF STEM Cs-corrected system equipped with a JEOL Centurio EDXS SDD spectrometer. The operating voltage was 80 kV. A Gatan Quantum ER Dual EELS system was used to obtain the EELS spectra and to estimate the sample thickness.

Grammage, thickness, breaking length, tensile, tear, bursting, and folding resistance were performed according to our previous study [14]. The grammage is the mass of the unit area of paper or paperboard determined by a specific test method. The breaking length was determined by using Electronic Testing System Instron 4411, according to Romanian ISO 1924-2:2009 standard. The bursting resistance was performed by using the Frank-Bursting Strength Tester 18530 F000 and according to Romanian SR EN ISO 2758:2015 standard. The folding endurance was determined by using the Schopper type equipment according to the Romanian standard SR ISO 5626:1996.

DSC was performed according to our previous study [14]. The degree of crystallinity (X_C) was determined as follows:

$$X_C = \frac{(\Delta H_m - \Delta H_{CC})}{\Delta H^{\circ}_m} \times 100, \tag{1}$$

where ΔH_m is melting enthalpy (J/g), ΔH_{CC} is enthalpy of cold crystallization (J/g), and ΔH°_m is enthalpy of crystalline fusion (i.e., 100% for PLA) (93 J/g) [15].

Oxygen transmission rate (OTR) was performed by coulometric sensor method. The film samples were cut using the template provided with the equipment. Before preparation, the film samples were conditioned in a desiccator containing anhydrous calcium chloride for a minimum of 48 hr. The film sample was fixed in the middle of test chamber to separate the chamber into upper room and lower room. When oxygen and nitrogen flow in upper and lower rooms, respectively, the oxygen molecules penetrate the film sample into the lower room and the coulometric sensor system detects and analyzes the oxygen content and calculates the OTR. When testing the container, oxygen is released outside and nitrogen inside of the container. The time required to reach steady state for OTR in sample was 64 hr.

FTIR, ash content, pH, electrical conductivity, and antioxidant activity were performed according to the procedure detailed in a study by Peter et al. [14]. Water vapor permeability (WVP) and grease permeability were determined

according to the procedure described in a study by Peter et al. [4].

The barrier properties against UV–vis light was determined by using the PerkinElmer Lambda 35 Spectrophotometer [9]. The experiment was performed in triplicate, and the opacity was determined by using the formula as follows:

$$\text{Opacity } (a.u. \text{ at } 600 \, nm/mm) = \frac{Abs \, at \, 600 \, nm}{x}, \qquad (2)$$

where Abs (absorbance) at 600 nm and x is film thickness (mm).

2.9. Statistical Analysis. The characterization experiments, as well as those corresponding to the curd storage, were performed in triplicate and the values were reported as mean, by using the Excel program. The level of significance was determined by using the Statistica 7.0 software (StatSoft, Inc., Tulsa, USA) and one-way analysis of variance (ANOVA—Tukey's test).

3. Results and Discussion

3.1. Characterization of the New and Recycled Nano-Ag-Graphene-TiO$_2$-PLA Film

3.1.1. Visual Appearance and Morphology of the Films. The visual appearance of the new and recycled films is shown in Table 1. The image of the new film clearly highlights the presence of composite particles, having different dimensions, unevenly dispersed in the PLA matrix. The macroscopic image of the recycled film is similar to that of the newly prepared film, that is, the composite particles distributed nonuniformly in the matrix and having different dimensions are observed.

Table 1 also shows the SEM images of the new and recycled samples. The observations are similar to those in macroscopic analysis, meaning that composite particles with dimensions of 10–20 nm in diameter are heterogeneously distributed in the network. No difference in the morphology as a result of the recycling procedure could be observed. The STEM microscopy performed in our previous study [4] showed that the Ag-graphene-TiO$_2$ composite contains titania and silver particles with approximately 20 and 5 nm in diameter, respectively, dispersed in the graphene matrix.

The elemental analysis of the recycled and the new film and of the neat PLA performed by EDXS analysis, as shown in Table 1, reveals that the difference of element content between the new and recycled film is statistically nonsignificant (one-way ANOVA—Tukey's test). In contrast, the elemental composition of the newly prepared composite differs significantly from that of the recovered composite (Figure 1) in terms of carbon content. The explanation is the degradation occurred by carbon during the thermal treatment.
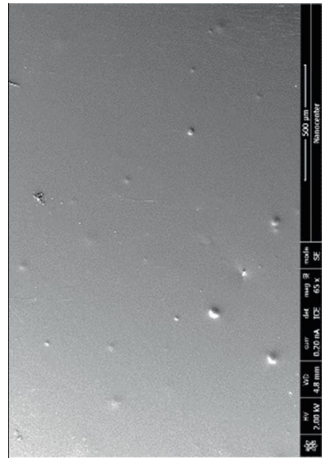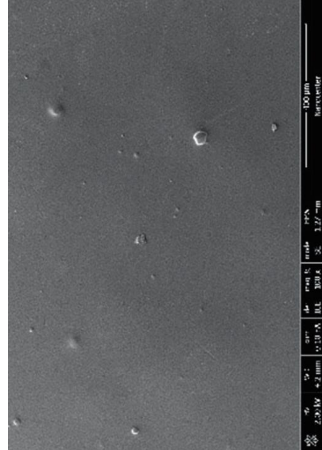
3.1.2. Thermal Transitions of the Films (DSC). Figures S1–S3 show the DSC thermograms of the new and recycled PLA-based and neat PLA films in which the thermal transitions of PLA are visible. The glass transition temperature (T_g) was observed at $60.2 \pm 2.2°C$ for neat PLA, at $58.1 \pm 3.3°C$ for new film, and at $59.7 \pm 4.8°C$ for the recycled film. An exothermic peak was formed at $121.9 \pm 9.2°C$ for the neat PLA, at $117.6 \pm 8.1°C$ for the new film, and at $95.2 \pm 3.4°C$ for the recycled film, due to the crystallization process of PLA, causing the reordering of the macromolecular chains from the PLA's matrix and leading to mobility after thermal treatment [16–18]. The endothermic peak corresponding to the melting process is visible at $150.5 \pm 4.4°C$ for neat PLA, $148.1 \pm 7.9°C$ for the new film, and at $178.6 \pm 10.2°C$ for the recycled film.

The incorporating Ag-graphene-TiO$_2$ composite nanoparticles slightly decreases the PLA's T_g from 60.2 to 58.1°C in the new film and to 59.7°C in the recycled film when compared to neat PLA (Table 2 and Figures S1–S3). This is explained by the PLA chain shrinkage assigned by the interconnectivity with the composite particles [19]. Similar results were obtained by Deghiche et al. [17] and Nomai et al. [19]. The crystallization temperature (T_{CC}) of neat PLA and the new film was similar (121.9 and 117.6°C, respectively), whereas that of the recycled film decreased to 95.2°C. The crystallization degree increases in the new and recycled films when compared to neat PLA because the composite nanoparticles act as nucleation centers [17]. It is a considerably difference of X_c between the new and recycled film, explained by the highly crystallized recovered composite, that induces a more considerable crystallization in the recycled film as in the new film. There are differences in T_{cc} and melting temperature (T_m), respectively, between the newly prepared film and the recycled film. Moreover, the new film has T_{cc} and T_m values closer to the unmodified PLA than the recycled film. These differences are due to the elementary composition of the newly prepared film different than that of the recovered film (Figures S1–S3). Also, differences between the composite structure from new and recycled film can be achieved in the FTIR spectra (Figure S4). It was previously mentioned that the recovered composite contains only traces of carbon, due to the heat treatment applied during the recovery, which demonstrates that the graphene has been degraded. The almost identical values of T_{cc} determined for neat PLA and new composite PLA demonstrate that the new Ag-graphene-TiO$_2$ composite did not induce significant structural changes of the polymer matrix because of the strong PLA's surface tension [20]. The significant decrease in the T_{cc} value (increase in T_m) achieved for recycled film demonstrates that the composition of the recovered material is structurally different from that of the new one and induced modifications in the PLA's surface tension and crystallization in a greater extent than in the newly prepared composite. Thus, it is inferred that the recovered composite is better incorporated into the PLA matrix than the new prepared one.

3.1.3. FTIR Spectroscopy of the Films. There are characteristic signals corresponding to PLA, TiO$_2$, and graphene in the FTIR spectra of the new and recovered PLA-based films, showing the formation of the chemical connections between the PLA and the composite (Figure S4 and Table 3). The signals at 2,973, 1,750, 1,451, 1,182–1,190, 1,081, and 867–689 cm^{-1}

TABLE 1: Images and elemental composition of the new and recycled nano-Ag-graphene-TiO$_2$-PLA films.

	New Ag-graphene-TiO$_2$-PLA	Recycled composite PLA	Neat PLA
Visual appearance			
SEM image			
C (wt%)	52 ± 5^a	58 ± 1^a	60 ± 1^a
O (wt%)	47 ± 4^a	42 ± 2^a	40 ± 1^a
Ti (wt%)	0.2 ± 0.01^a	0.11 ± 0.01^a	–
Ag (wt%)	0.1 ± 0.01^a	0.1 ± 0.01^a	–

In each line, mean values with superscript letter ([a]) are statistical nonsignificant different at $p < 0.01$ (one-way ANOVA—Tukey's test).
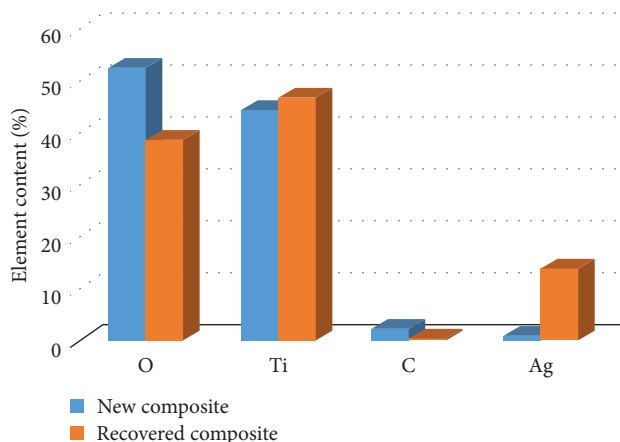
FIGURE 1: Elemental composition of the new and recovered Ag-graphene-TiO$_2$ nanocomposite.

TABLE 2: Thermal properties of the films.

Sample	T_g (°C)	T_{CC} (°C)	T_m (°C)	ΔH_{CC} (J/g)	ΔH_m (J/g)	Xc
Neat PLA	60.2 ± 2.2[a]	121.9 ± 9.2[a]	150.5 ± 4.4[a]	17.0 ± 0.7[a]	17.12 ± 5.1[a]	0.129 ± 0.001[a]
New film	58.1 ± 3.3[a]	117.6 ± 8.1[b]	148.1 ± 7.9[b]	15.1 ± 1.1[b]	17.2 ± 5.3[a]	2.258 ± 1.7[b]
Recycled film	59.7 ± 4.8[b]	95.2 ± 3.4[c]	178.6 ± 10.2[c]	21.2 ± 1.9[c]	32.2 ± 3.9[b]	11.827 ± 4.8[c]

T_g, glass transition temperature; T_{CC}, crystallization temperature; T_m, melting temperature; ΔH_{CC}, enthalpy of cold crystallization; ΔH_m, melting enthalpy. In each line, mean values with superscript letters ([a,b,c]) are statistical nonsignificant different at $p < 0.01$ (one-way ANOVA—Tukey's test).

TABLE 3: Specific signals and description from the FTIR spectra.

Peak (cm^{-1})	New film	Recycled film	Neat PLA	Description
2,973	√	√	√	Stretching vibration of aliphatic methyl groups from PLA [17]
1,750	√	√	√	Stretching vibration of the C=O bond from the ester group from PLA
1,451	√	√	√	[17, 21]
1,395	–	√	–	Vibration of —Ti—O—C bonds between recovered composite and PLA
1,382	√	–	√	—O—C—O— stretching from PLA [22]
1,368	–	√	–	Vibration of —Ti—O—C bonds between recovered composite and PLA
1,303	√ (small)	√	–	Stretching of —Ti—O—C included in the PLA matrix
1,182–1,190	√	√	√	—C—O— stretching from PLA [17]
1,127 and 1,044	√ (shoulder)	√	–	Presence of composite into the PLA matrix
1,081	√	√	√	Vibration of —O—CH—CH$_3$ from PLA [17]
952	√ (small)	√	√ (small)	Presence of composite into the PLA matrix
867	√	√	√	Vibration of C—C bond from the —C—COO— in PLA [21] Vibration of
751	√	√	√	Ti—O—Ti and C—O—Ti [23]
689	√	√	√	

found in all FTIR spectra are characteristic to the vibration of specific bonds in the PLA skeleton [17, 21].

Specific signals assigned by the composite presence can be found at 1,382, 1,303, 1,127, 1,044, and 952 cm^{-1} and are assigned by the stretching of the Ti—O—C connections [22, 23]. Moreover, the formation of these C—O—Ti bonds is also demonstrated by the signals in the range of 600–900 cm^{-1} that overlaps with those of PLA.

The FTIR spectra of the new film and of the recycled film are different in the regions at 1,368–1,395, 1,303, 1,127, 1,044, and 952 cm^{-1}. Thus, the peak at 1,382 cm^{-1} from the FTIR spectra of new film and of PLA is splitted in two

peaks at 1,395 and 1,368 cm^{-1} found in the FTIR spectrum of recovered film. The peaks at 1,303, 1,127, 1,044, and 952 cm^{-1} are small in the FTIR spectrum of the new film but become stronger in that of the recovered film. These peaks are assigned to the interconnection of PLA with the TiO$_2$ network and the formation of C—O—Ti bridges [23] and the different signal intensities demonstrate the different structures of the recovered composite in comparison with the new one.

These observations are supported by the DSC results, which showed that the recycled composite, due to its different compositions in comparison with the new one, altered

Table 4: Characteristics of the new and recycled nano-Ag-graphene-TiO$_2$-PLA films.

Characteristic		New film	Recycled film	Neat PLA
Grammage (g/m^2)		39.6 ± 8.54[a]	41.66 ± 5.68[a]	40.95 ± 4.24[a]
Thickness (μm)		79 ± 2.57[a]	75 ± 0.87[a]	23 ± 1.68[b]
Breaking length (%) according to SR EN ISO 1924-2:2009		4.11 ± 0.45[a]	6.19 ± 0.42[b]	15.28 ± 2.45[c]
Tearing resistance (mN) according to SR EN ISO 1974:2012		120 ± 5.46[a]	190 ± 4.23[b]	100 ± 3.61[a]
Slashing resistance (kPa) according to SR EN ISO 2758:2015		167 ± 5.89[a]	207 ± 4.28[b]	135 ± 5.63[c]
Folding resistance (no.) according to SR ISO 5626:1996		3,484 ± 21[a]	3,998 ± 35[b]	3,452 ± 42[a]
Oxygen transmission rate (OTR) (cm^3/m^2 × day)		480 ± 156[a]	393 ± 89[b]	719 ± 91[c]
Opacity (a.u. at 600 nm)		0.328 ± 0.013[a]	0.304 ± 0.013[a]	0.921 ± 0.56[b]
Ash (%)		0.49 ± 0.0045[a]	0.4 ± 0.088[a]	0.03 ± 0.001[b]
pH		5.86 ± 0.04[a]	5.72 ± 0.089[a]	5.91 ± 0.09[a]
Electrical conductivity (μS/cm)		26.43 ± 3.15[a]	33.3 ± 7.23[b]	13.2 ± 5.82[c]
Water vapor permeability (WVP) (g/s m Pa) × 10^{10}		6.903 ± 0.85[a]	7.98 ± 1.05[b]	3.13 ± 0.85[c]
Grease permeability (%)		0	0	0
Antioxidant activity (%)		13.3 ± 0.24[a]	10.15 ± 0.37[b]	14.57 ± 0.26[c]
Solubility in simulant A (distilled water) (%)	20°C	5.54 ± 0.54[a]	0.4 ± 0.01[b]	3.52 ± 0.57[c]
	4°C	8.6 ± 0.79[a]	2.4 ± 0.08[b]	3.99 ± 0.42[c]
Solubility in simulant B (acetic acid 3%) (%)	20°C	5.54 ± 0.42[a]	12.1 ± 1.47[b]	3.36 ± 0.42[c]
	4°C	7.81 ± 1.23[a]	6.2 ± 0.21[b]	1.91 ± 0.21[c]
Solubility in simulant C (ethanol 65%) (%)	20°C	3.8 ± 0.22[a]	1 ± 0.04[b]	3.61 ± 0.47[c]
	4°C	3.5 ± 0.24[a]	5.9 ± 0.99[b]	4.28 ± 0.98[c]

In each line, mean values with different letters ([a,b,c]) are significantly different at $p < 0.01$ (one-way ANOVA—Tukey's test).

the PLA's surface tension and induced more efficient chemically connections with the PLA chain.

3.1.4. Physical–Chemical and Biochemical Characteristics of the Films. The characteristics of the new and recycled film in comparison with neat PLA are shown in Table 4. The difference between the two film types and neat PLA in terms of grammage, pH, and fat permeability is statistically nonsignificant. However, the opacity and the ash content variation are also statistically nonsignificant when comparing the new film with the recycled film.

In contrast, the difference of mechanical characteristics, OTR, WVP, solubility in food simulants, electrical conductivity, and antioxidant activity is statistically significant in a quantum higher than 99% ($p < 0.01$, one-way ANOVA—Tukey's test) between new and recycled films.

The largest tear elongation was determined for neat PLA, 73% and 59% higher than for the newly prepared film and for the recycled film, respectively. When comparing the modified films, it can be observed that the tear elongation of the recycled film is 50% higher than of the new film.

All the other mechanical strength parameters of the recycled film are superior to those of the new film: the tear resistance is 58.33% higher, the burst resistance is 24% higher, and the bending resistance is 14.7% higher. The increase in mechanical resistance properties as a result of the PLA's additivation was also reported in literature, following the addition of multiscale cellulosic biocomposites [21], chitosan [24], or halloysite nanotubes [25]. The mechanical resistance of the recycled film is higher than of the new and unmodified PLA film and is explained by the multitude of

new bonds arising between the PLA network and the composite particles, proven by the FTIR spectroscopy analysis, i.e., O—C—O— and —Ti—O—C—PLA bonds (Figure S4 and Table 3), which physical hydrogen bonds are added to [25]. All of these bonds restrict the mobility of PLA chains, increase its strength, and ensure the matrix's rigidity. This explains why the elongation at break of the modified film is much lower in comparison to that of the neat PLA.

OTR of the modified films has decreased considerably by 33% (in the new film) and 45% (in the recycled film), respectively, compared to PLA (Table 4). Among the modified films, OTR of the recycled film is 18.1% lower than of the new film. This is correlated with the mechanical resistance characteristics, i.e., the recycled film is least permeable for oxygen and the most mechanically resistant due to the compaction of the composite PLA network in a greater extent than in the case of the new prepared film (Table 4). Subsequently, this is a result of different chemical compositions and structures of the recovered composite when compared to the new one, a fact confirmed by the EDXS results. The presence of the graphene network in the newly prepared film affects its structure, in that, having a non-polar character, the carbon network creates, together with the non-polar methyl groups of PLA, repulsions that make the matrix unable to compact.

The WVP of the new and recovered films is 2.2 and 2.5 times, respectively, higher than that of PLA's (Table 4). This is a negative aspect explained by the elemental composition and structure of the new prepared composite different from the recovered one. In the newly prepared composite, the presence of graphene inserted in the PLA's network provides

added hydrophobic role to the composite matrix. Instead, in the recycled film, graphene was broken down during the recovery; thus, Ti, Ag, and traces of C remained only and the hydrophobic supply was considerably reduced.

The antioxidant activity of the modified films is lower than that of the unmodified films, and, moreover, that of the recycled film is smaller than that of the newly prepared film.

In general, the solubility in food simulants of the recycled film is lower than that of the newly prepared film, even that of the unmodified one, which is also explained by the composite network different from that of the newly prepared film. So, it can be appreciated that the mechanical resistance, oxygen barrier, and food simulants properties of the recycled film are superior to the newly prepared film, due to the fact that another type of composite with different elemental compositions was obtained during the recovery procedure, that created superior qualitative and quantitative connections in the PLA matrix. This was also supported by DSC and FTIR results.

The behavioral difference between the newly prepared film and the recycled film lies in the following mechanism. The chemical reactivity and kinetic stability of the component phases from the film and the composite are explained by the electron occupation of HOMO and LUMO molecular orbitals. HOMO is the most electron-occupied molecular orbital, and LUMO is the poorest in electrons. Reactivity is due to the ability of electrons to be transferred from HOMO to LUMO and increases with the reduction of the energy difference between HOMO and LUMO. In PLA, HOMO is located in the carbonyl groups $C = O$, which are the most reactive and serve as electron donors [17]. In TiO_2, HOMO and LUMO are found in the titanium atoms and act as electron acceptors. In graphene, HOMO is in the carbon cycles and acts as electron donors [26]. In the new film Ag-graphene-TiO_2-PLA (Figure 2a), as reported, there are reactive and polar areas (carbonyl groups) but also nonpolar areas (methyl groups). The carbonyl reactive areas, which act as electron donors, transfer the electrons to the Ti atoms (pathway A), by activating them, as the graphene network attached to the semiconductor (pathway B). The two pathways of TiO_2 activation are also added to photochemical activation under the action of UV radiation in the solar spectrum (pathway C) [27]. Ag nanoparticles attached to the TiO_2 network stimulate the electronic transfer, reduce the recombination of charge carriers, and initiate the reduction processes. The electrons activated by the nano-Ag can, subsequently, be involved in two ways: (1) reduce the carbocations in the PLA structure, formed due to the polarization of the carbonyl bond, generating oxygen anions that alter the PLA's surface state and affect its surface tension, as demonstrated by the DSC results and (2) reduce species in the environment surrounding the film. Also, the connection of the PLA network with TiO_2 is made by a considerably number of hydrogen bonds [17, 28]. The presence of the graphene network in the newly prepared film has a disadvantage, namely the fact that having a nonpolar character, the carbon network creates, next to the nonpolar methyl groups of PLA, repulses that make the matrix unable to compact. This disadvantage is considerably reduced in the recycled film (Figure 2b) due to the graphene's very low concentration. This explains why the recycled film has superior mechanical properties to the newly prepared film. Moreover, the active carbonyls from the proximity of TiO_2 and Ag active centers stimulate the electronic transfer and intensify the formation of reactive oxygen anions, demonstrated by appearing of new peaks in the FTIR spectrum of the recovered film.

4. Results of Curd Packaging in the New and the Recycled Films

4.1. Visual Appearance of the Curd Cheese. The curd cheese samples packed in each of the three types of packaging did not change from the organoleptical point of view during 14 days of refrigeration (Tables 5 and 6).

From day 14 to 21, significant organoleptic changes have occurred, especially in the case of the cheese kept in the neat PLA. Thus, after 14 days of storage, a positive influence of the modified PLA on the cheese's organoleptical properties has been observed in comparison to that of the sample from the unchanged PLA, assigned by the presence of the composite Ag-graphene-TiO_2. The photocatalytic activity of TiO_2 [4] and the antimicrobial efficiency of Ag and graphene are already known [14, 19, 20, 24]. The cheese in PLA changed its color from white to yellow, became crumbling and acquired, a strong fermented smell. In contrast, the new film sample removed a little whey during storage and became yellowish. The sample in the recycled film suffered the fewest changes after 21 days of storage. So, from the organoleptic point of view, PLA and the newly prepared film ensure a shelf life of 14 days for cheese and the recycled one of 21 days, according to SR3664:2008.

4.2. Physical–Chemical Characterization of the Curd Cheese Wrapped in the New and Recycled Films. The variation of the physical–chemical parameters of the curd cheese kept in the investigated films is shown in Figure 3(a)–3(e). The monitored parameters are standardized according to the Romanian SR 3664 from 2008 in force, namely mass loss, titratable acidity, dry mass, and fat and protein contents.

When taking into account the values obtained at each time interval, the one-way ANOVA analysis—Tukey's test model showed that the variation of mass loss (Figure 3(a)), dry matter (Figure 3(c)), fat (Figure 3(d)), and protein (Figure 3(e)) of the curd cheese, depending on the wrapping material, is statistically insignificant.

If only 21-day values were taken into account, differences in the mass loss of cheese samples packed in the three package types were statistically significant higher than 99%, while those corresponding to the dry matter were statistically nonsignificant. The differences in fat content are statistically nonsignificant when compared to the sample wrapped in the recycled film and in the newly prepared film, respectively, but that between the sample from newly prepared film and that stored in the unchanged PLA is significant (>99%).

When considering the protein variation as a function of the film type, at 21 days, the difference between the sample in the recycled film and that from the newly prepared film is
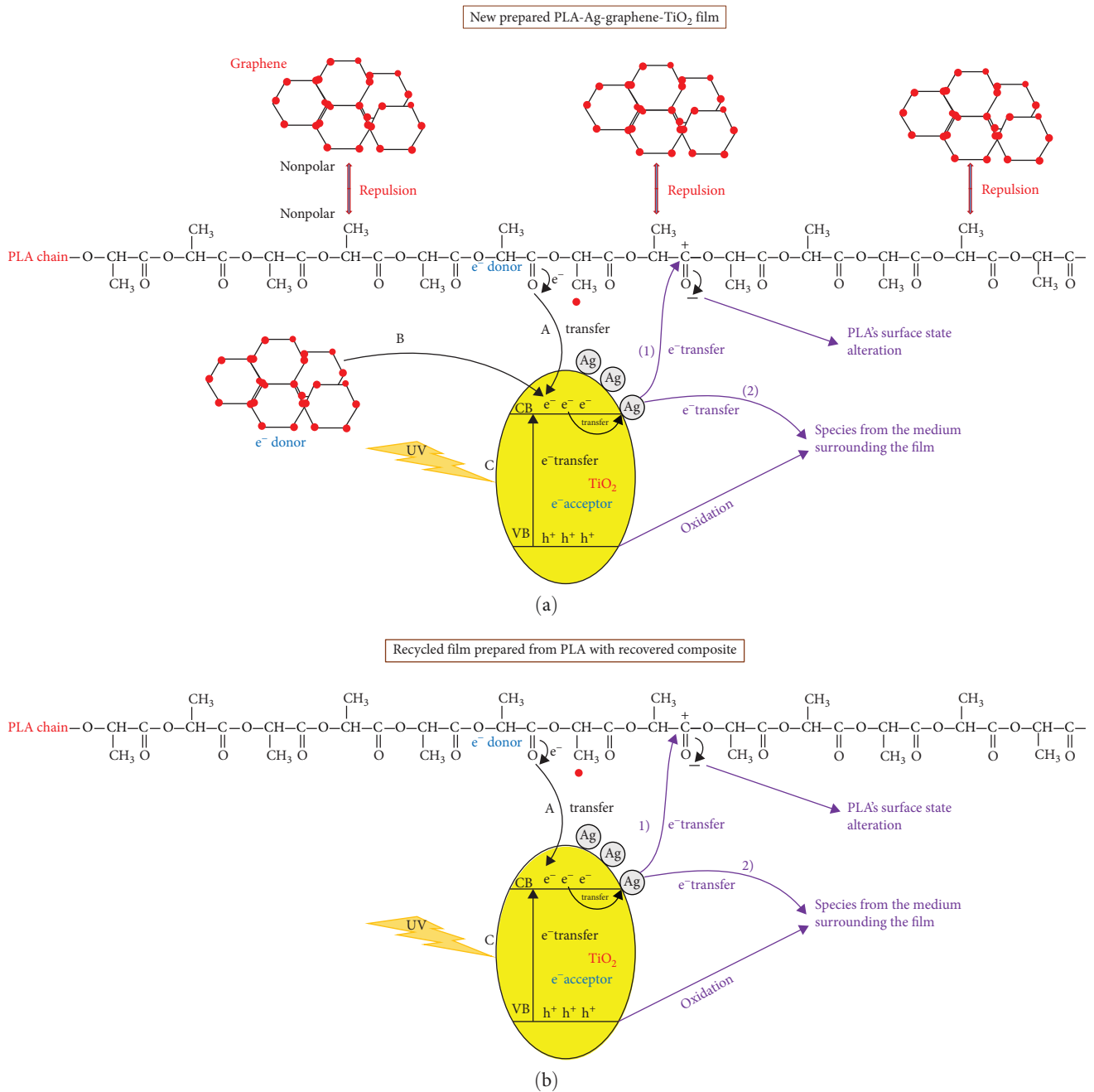
FIGURE 2: Bonds formation in the new prepared film (a) and recycled film (b).

significant (>95%), as well as that between the cheese from recycled film and neat PLA.

The highest variation in the mass loss after 21 days of storage was registered in the curd cheese kept in the new film (11.6%) and the lowest in that kept in the recycled film (4.6%). The most accentuated decrease in fat content occurred in curd cheese kept in the neat PLA (10.23%), while the lowest in the recycled film (1.63%).

The same variation was determined for the protein content, so the protein was the most severely degraded during the storage in the neat PLA and in the new film (25.35%) and the least affected during the cheese packaging in the recycled film (17.2%). The highest capacity to preserve the protein content was provided by the recycled film, as a result of the film structure and the most intense degree of compaction (Figure 2(b)) compared to the newly prepared film (Figure 2(a)). Thus, the OTR and solubility (Table 4) of the recycled film significantly lower in comparison to the newly prepared film, reduced the oxygen penetration and the film dissolution, respectively, and implicitly the intensity of oxidative processes in the intrapackaging space.

When analyzing the curd cheese's titratable acidity as a function of the packaging material (Figure 3(b)), it is noticed that variation of the acidity from the recycled film is

TABLE 5: Visual appearance of the curd cheese wrapped in the new and recycled films and neat PLA under refrigeration.

Period (day)	New film	Recycled film	Neat PLA
0			
7			
14			

Table 5: Continued.

Period (day)	New film	Recycled film	Neat PLA
21			

TABLE 6: Organoleptic properties of the curd cheese stored in the new and recycled films and neat PLA under refrigeration, established based on the Romanian Quality Standard for fresh cheese SR3664:2008.

| Period (day)	Characteristics	New film	Recycled film	Neat PLA
0 and 7	Appearance	Homogeneous, clean paste without whey leakage		
	Consistency	Fine paste with a low grounty consistency		
	Color	White		
	Flavor	Pleasant		
	Taste	Pleasant, taste of lactic fermentation, with no foreign tastes (acidic, bitter, of mold and yeast, smocked, etc.)		
14	Appearance	No changes when compared with those from day 0		
	Consistency			
	Color			
	Flavor			
	Taste			
21	Appearance	Homogeneous, with a very reduced whey leakage		Homogeneous, with whey leakage
	Consistency	Slightly crumbling	Fine paste	Crumbling
	Color	White-yellowish	White	Yellowish
	Flavor	A little bit pungent	Pleasant, with no foreign tastes	Acidic and of yeasts
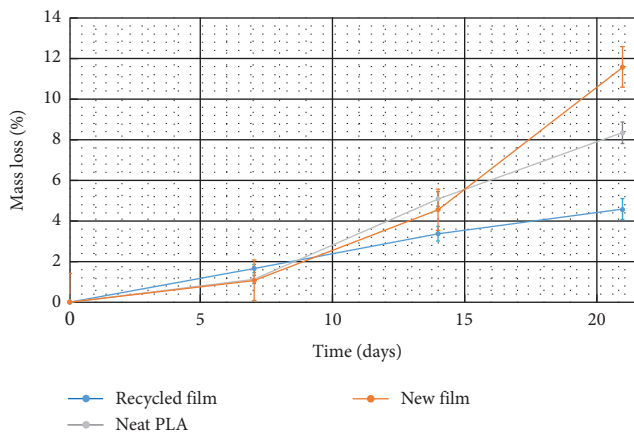
(a)
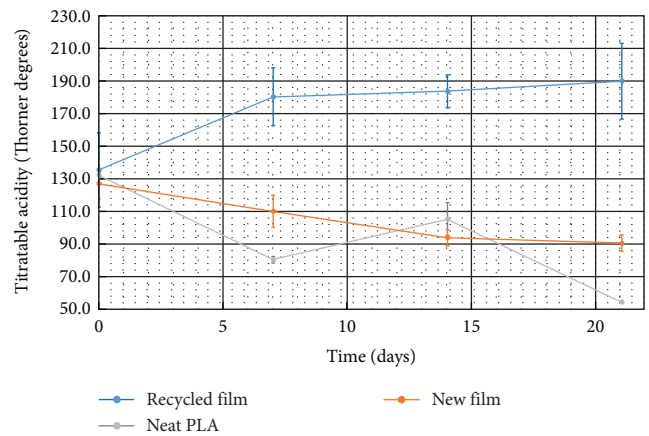
(b)
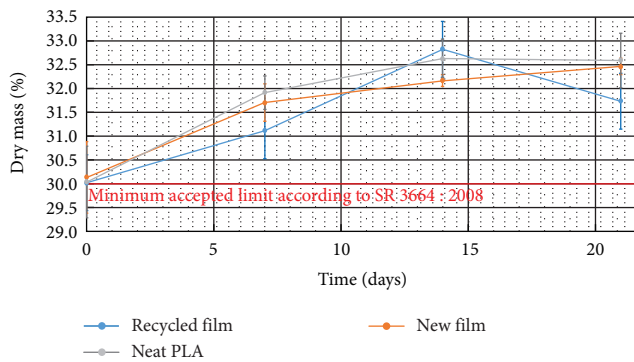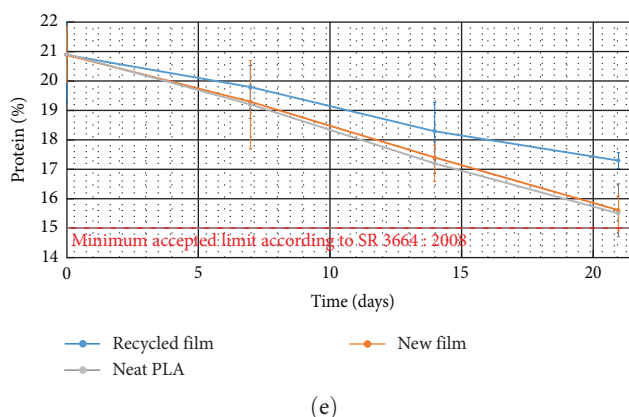
(c)
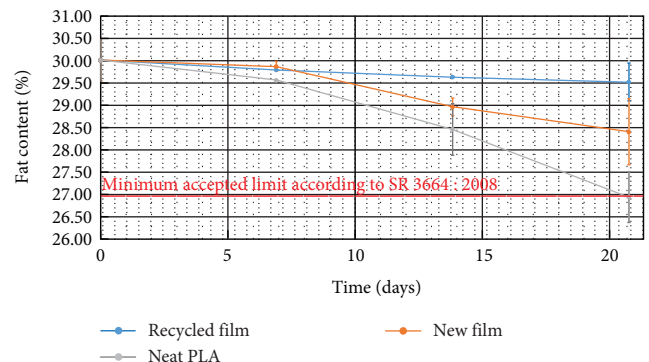
(d)

FIGURE 3: Continued.

(e)

Figure 3: Physical–chemical parameters of the curd stored in the recycled and new films and in neat PLA: (a) mass loss, (b) titratable acidity, (c) dry mass, (d) fat, and (e) protein.

significant in comparison with that from the new film during 21 days of storage ($p < 0.05$). However, the acidity evolution of the cheese from new film and the neat PLA is statistically nonsignificant. Thus, the acidity of the cheese kept in the recycled film increased by 40.5% after 21 days of refrigeration, while in the case of the new film and neat PLA, it decreased by 28.8% and 59.1%, respectively. The rise of acidity during storage was also reported by Jafarzadeh et al. [29] who coated active edible film based on whey protein modified with white tea extract on the fresh cottage cheese. This behavior could be explained by the fact that the recycled packaging film did not affect the functionality of lactic bacteria, as the newly prepared film or neat PLA. This is due to the different compositions of the recycled composition and the different structures of the recycled film compared to the new one, demonstrated by DSC and FTIR analyses and illustrated in mechanism, as shown in Figures 2(a) and 2(b). The maximum accepted limit of titratable acidity and the minimum accepted limit of dry matter, fat, and protein according to SR 3664:2008 have not been reached in the case of any cheese sample, so the curd cheese can be stored safely for 21 days in all three types of studied packaging materials.

Paulsen et al. [30] who monitored the evolution of broccoli under three different storage conditions (LLDPE packaging, biodegradable packaging containing PBAT/PLA, and unpackaged) demonstrated that the smallest changes in organoleptic characteristics, mass loss, oxygen and carbon dioxide evolution, firmness, chlorophyll, and carotenoid content of broccoli were recorded during its storage in LLDPE and in biodegradable film, highlighting that the PBAT/PLA has similar conservation characteristics to LLDPE and is also biodegradable.

Zheng et al. [31] have successfully obtained active films containing a cocktail of biodegradable materials (PBPA, PLA, PCL) modified with TiO_2 and natamycin, with mechanical and microbiological properties superior to the conventional films and showed their strong preservative effect on the grapes. After 30 days of storage at 0.5°C, the grapes kept in active packaging did not change their organoleptic properties compared to day 0, but the nonmodified grapes were deeply altered.

Both the results of structural, thermal, and mechanical resistance analyses and the results obtained when storing cheese demonstrate that the recycled film has a more conservative role on the cheese than the newly prepared one, which further encourages the recycling.

5. Conclusions

The study aims to assess the structural, morphological, mechanical resistance, physical–chemical and biochemical characteristics, as well as the preservative role on curd cheese of a recycled PLA film, obtained by recovering the nano-Ag-graphene-TiO_2 composite from the used PLA-based film, followed by its incorporation in the new PLA network. Visually, the recycled film looked just like the new one. The elementary quantitative analysis of the newly prepared and the recovered Ag-graphene-TiO_2 composite, used as active compound in the PLA film, showed that the graphene was carbonized during the recovery procedure, so the newly prepared composite is compositionally different from the newly prepared one. This induced variable DSC and FTIR results was manifested by: (1) higher crystallization of the recycled film network than the newly prepared one, (2) recovered composite reduced the surface tension of the PLA in a higher extend than the newly prepared composite, which showed that the recovered composite is better incorporated into the PLA network, and (3) new bonds appear in the recycled film, which also demonstrates that the recycled film is more compact than the new one. The mechanical and barrier resistance properties of the recycled film superior to the newly prepared one are due to the new connections appeared in the matrix following recycling, ensuring a high compaction degree. The curd cheese has been successfully stored in the recycled packaging for 21 days, the organoleptic characteristics being superior to those of cheese kept in new film or neat PLA. The recycled packaging reduced the protein degradation of cheese by 8% compared to the newly prepared one. The study shows that the recycling procedure was a success

from two points of view: (1) packaging waste reduction and (2) production of packaging material with a preservative action even more efficient than the newly prepared film.

Data Availability

All the data that make the subject of the manuscript results are available on request.

Conflicts of Interest

The authors declare that there are no conflicts of interest regarding the publication of this paper.

Authors' Contributions

Anca Peter—conception, experimental design, and writing; Anca Mihaly Cozmuta—carrying out measurements and visualization; Leonard Mihaly Cozmuta—statistical analysis; Nicula Camelia—methodology and visualization; Goran Drazic, Antonio Penas, and Stefania Silvi—supervision.

Acknowledgments

Supplementary Materials

Figure S1: differential scanning calorimetry (DSC) curves of new prepared nano-Ag-graphene-TiO$_2$-PLA films. Figure S2: differential scanning calorimetry (DSC) curves of recycled nano-Ag-graphene-TiO$_2$-PLA films. Figure S3: differential scanning calorimetry (DSC) curves of neat PLA film. Figure S4: FTIR spectra of the new and recycled nano-Ag-graphene-TiO$_2$-PLA films and of neat PLA. (*Supplementary Materials*)

References

[1] R. Plavec, S. Hlaváčiková, L. Omaníková et al., "Recycling possibilities of bioplastics based on PLA/PHB blends," *Polymer Testing*, vol. 92, Article ID 106880, 2020.

[2] M. Ramos, E. Fortunati, M. Peltzer, A. Jimenez, J. M. Kenny, and M. C. Garrigos, "Characterization and disintegrability under composting conditions of PLA-based nanocomposite films with thymol and silver nanoparticles," *Polymer Degradation and Stability*, vol. 132, pp. 2–10, 2016.

[3] N'Afifah Zabidi, F. Nazri, I. S. M. A. Tawakkal, M. S. M. Basri, R. K. Basha, and S. H. Othman, "Characterization of active and pH-sensitive poly(lactic acid) (PLA)/nanofibrillated cellulose (NFC) films containing essential oils and anthocyanin for food packaging application," *International Journal of Biological Macromolecules*, vol. 212, pp. 220–231, 2022.

[4] A. Peter, L. M. Cozmuta, C. Nicula et al., "Chemical and organoleptic changes of curd cheese stored in new and reused active packaging systems made of Ag-graphene-TiO$_2$-PLA," *Food Chemistry*, vol. 363, Article ID 130341, 2021.

[5] H. Chi, S. Song, M. Luo et al., "Effect of PLA nanocomposite films containing bergamot essential oil, TiO$_2$ nanoparticles, and Ag nanoparticles on shelf life of mangoes," *Scientia Horticulturae*, vol. 249, pp. 192–198, 2019.

[6] S. Geetha, A. Thangamani, R. Valliappan, S. Vedanayaki, and A. Ganapathi, "Sulfated titania (TiO$_2$–SO$_4^{2-}$) as an efficient and reusable solid acid catalyst for the multi-component synthesis of highly functionalized piperidines," *Chemical Data Collections*, vol. 30, Article ID 100565, 2020.

[7] N. G. Menon, L. George, S. S. V. Tatiparti, and S. Mukherji, "Efficacy and reusability of mixed-phase TiO$_2$–ZnO nanocomposites for the removal of estrogenic effects of 17β-Estradiol and 17α-Ethinylestradiol from water," *Journal of Environmental Management*, vol. 288, Article ID 112340, 2021.

[8] H. Yan, R. Wang, R. X. Liu et al., "Recyclable and reusable direct Z-scheme heterojunction CeO$_2$/TiO$_2$ nanotube arrays for photocatalytic water disinfection," *Applied Catalysis B: Environmental*, vol. 291, Article ID 120096, 2021.

[9] Y. Liu, Y. Xiang, H. Xu, and H. Li, "The reuse of nano-TiO$_2$ under different concentration of CO$_3^{2-}$ using coagulation process and its photocatalytic ability in treatment of methyl orange," *Separation and Purification Technology*, vol. 282, Part B, Article ID 120152, 2022.

[10] A. Khodanazary and B. Mohammadzadeh, "The effects of polylactic acid-whey protein isolated bi-layer film incorporated with ZnO nanoparticles on the quality of common carp *Cyprinus carpio*," *Journal of Food Measurement and Characterization*, vol. 17, pp. 4684–4694, 2023.

[11] F. Izadi, M. Pajohi-Alamoti, A. Emamifar, and A. Nourian, "Fabrication and characterization of active poly(Lactic Acid) films containing *Thymus daenensis* essential oil/Beta-cyclodextrin inclusion complex and silver nanoparticles to extend the shelf life of ground beef," *Food and Bioprocess Technology*, 2023.

[12] K. Poonsawat and M. Seadan, "Determination of molecular weight and molecular weight distribution of poly(lactic acid) by dynamic mechanical properties of polymer in melted state," poster accessed Aug 11 2023 http://www.dpst.sc.su.ac.th/assets/news/poster-stcy11/Determination.pdf.

[13] A. Peter, L. M. Cozmuta, C. Nicula et al., "Recovery and characterization of nano-Ag-graphene-TiO$_2$ - active compound from polylactic acid (PLA)-based film," *Journal of Polymers and the Environment*, 2023.

[14] A. Peter, L. M. Cozmuta, C. Nicula et al., "Morpho-structural and chemical characterization of paper based materials with functionalized surface," *Materials Chemistry and Physics*, vol. 267, Article ID 124693, 2021.

[15] I. Mayouf, M. Guessoum, M. Fuensanta, and J. M. M. Martìnez, "Appraisal of ε-caprolactam and trimellitic anhydride potential as novel chain extenders for poly (lactic acid)," *Polymers Engineering and Science*, vol. 60, no. 5, pp. 944–955, 2020.

[16] J. Gómez-Estaca, P. Montero, F. Fernández-Martín, A. Alemán, and M. C. Gómez-Guillén, "Physical and chemical properties of tuna-skin and bovine hide gelatin films, with added aqueous oregano and rosemary extract," *Food Hydrocolloids*, vol. 23, no. 5, pp. 1334–1341, 2009.

[17] A. Deghiche, N. Haddaoui, A. Zerriouh et al., "Effect of the stearic acid-modified TiO$_2$ on PLA nanocomposites: morphological and thermal properties at the microscopic scale," *Journal of Environmental Chemistry Engineering*, vol. 9, no. 6, Article ID 106541, 2021.

[18] S. E. Fenni, O. Monticelli, L. Conzatti et al., "Correlating the morphology of poly(L-lactide)/poly(butylenes succinate)/graphene oxide blends nanocomposites with their

crystallization behavior," *Express Polymers Letters*, vol. 12, no. 1, pp. 58–70, 2018.

[19] J. Nomai, B. Suksut, and A. K. Schlar, "Crystallization behavior of poly(lactic acid)/titanium dioxide nanocomposites," *KMUTNB International Journal of Applied Science and Technology*, vol. 8, no. 4, pp. 251–258, 2015.

[20] Y.-B. Luo, W.-D. Li, X.-L. Wang, D.-Y. Xu, and Y.-Z. Wang, "Preparation and properties of nanocomposites based on poly (lactic acid) and functionalized TiO_2," *Acta Materialia*, vol. 57, no. 11, pp. 3182–3191, 2009.

[21] M. A. Ruz-Cruz, P. J. Herrera-Franco, E. A. Flores-Johnson, M. V. Moreno-Chulim, L. M. Galera-Manzano, and A. Valadez-Gonzalez, "Thermal and mechanical properties of PLA-based multiscale cellulosic biocomposites," *Journal of Material Research Technology*, vol. 18, pp. 485–495, 2022.

[22] R. Atchudan, T. N. J. I. Edison, S. Perumal, D. Karthikeyan, and Y. R. Lee, "Effective photocatalytic degradation of anthropogenic dyes using graphene oxide grafting titanium dioxide nanoparticles under UV-light irradiation," *Journal of Photochemistry and Photobiology A: Chemistry*, vol. 333, pp. 92–104, 2017.

[23] Q. Zhang, N. Bao, X. Wang et al., "Advanced fabrication of chemically bonded graphene/TiO_2 continuous fibers which enhanced broadband photocatalytic properties and involved mechanisms exploration," *Scientific Reports*, vol. 6, Article ID 38066, 2016.

[24] M. Râpă, A. C. Miteluţ, E. E. Tănase et al., "Influence of chitosan on mechanical, thermal, barrier and antimicrobial properties of PLA-biocomposites for food packaging," *Composites Part B: Engineering*, vol. 102, pp. 112–121, 2016.

[25] N. P. Risyon, S. J. Othmana, R. K. Bashaa, and R. A. Talib, "Characterization of polylactic acid/halloysite nanotubes bionanocomposite films for food packaging," *Food Packaging and Shelf Life*, vol. 23, Article ID 100450, 2020.

[26] A. Bayat and E. Saievar-Iranizad, "Synthesis of green-photoluminescent single layer graphene quantum dots: determination of HOMO and LUMO energy states," *Journal of Luminescence*, vol. 192, pp. 180–183, 2017.

[27] L. Baia, A. Peter, V. Cosoveanu et al., "Synthesis and nanostructural characterization of TiO_2 aerogel for photovoltaic devices," *Thin Solid Films*, vol. 511-512, pp. 512–516, 2006.

[28] K. P. Cresnar, L. K. Zemlji, L. Papadopoulos et al., "Effects of Ag, ZnO and TiO_2 nanoparticles at low contents on the crystallization, semicrystalline morphology, interfacial phenomena and segmental dynamics of PLA," *Material Today Communications*, vol. 27, Article ID 102192, 2021.

[29] S. Jafarzadeh, A. Salehabadi, A. M. Nafchi, N. Oladzadabbasabadi, and S. M. Jafari, "Cheese packaging by edible coatings and biodegradable nanocomposites; improvement in shelf life, physicochemical and sensory properties," *Trends in Food Science & Technology*, vol. 116, pp. 218–231, 2021.

[30] E. Paulsen, P. Lema, D. Martínez-Romero, and C. García-Viguera, "Use of PLA/PBAT stretch-cling film as an ecofriendly alternative for individual wrapping of broccoli heads," *Sciencia Horticulturae*, vol. 304, Article ID 111260, 2022.

[31] Y. Zheng, X. Jia, Z. Zhao et al., "Innovative natural antimicrobial natamycin incorporated titanium dioxide (nano-TiO_2)/poly (butylene adipate-co-terephthalate) (PBAT) /poly (lactic acid) (PLA) biodegradable active film (NTP@PLA) and application in grape preservation," *Food Chemistry*, vol. 400, Article ID 134100, 2023.